

# Above-Room-Temperature Magnetodielectric Coupling in a Possible Molecule-Based Multiferroic: Triethylmethylammonium Tetrabromoferrate(III)

Hong-Ling Cai,<sup>†</sup> Yi Zhang,<sup>†</sup> Da-Wei Fu,<sup>†</sup> Wen Zhang,<sup>†</sup> Tao Liu,<sup>‡</sup> Hirofumi Yoshikawa,<sup>§</sup> Kunio Awaga,<sup>§</sup> and Ren-Gen Xiong<sup>\*,†</sup>

<sup>†</sup>Ordered Matter Science Research Center, Southeast University, Nanjing 211189, P.R. China

<sup>‡</sup>State Key Laboratory of Fine Chemicals, Dalian University of Technology, Dalian 116012, P.R. China

<sup>§</sup>Research Center for Materials Science and Department of Chemistry, Nagoya University, Nagoya 464-8602, Japan

**S** Supporting Information

**ABSTRACT:** A possible above-room-temperature molecular multiferroic, triethylmethylammonium tetrabromoferrate(III) (**1**), has been discovered. Its ferroelectric and magnetic phase transitions take place at almost the same temperature ( $\sim 360$  K), resulting in strong magnetodielectric (MD) coupling, with a MD ratio of 18% at 0.6 MHz. Interestingly, **1** also undergoes a low-temperature ferroelectric–ferroelectric phase transition with an Aizu notation of  $6mmF6$  and small magnetic and dielectric anomalies at 171 K.

Multiferroics, a term that refers to materials having two or three different switchable ferroic orders at the same time, i.e., ferromagnetism, ferroelectricity, and ferroelasticity, have attracted much research interest due to their potential applications in memory storage devices, ferroelectric field-effect transistors, and optoelectronic devices.<sup>1</sup> On the other hand, magnetoelectric coupling effects (including magnetodielectric and magnetocapacitance) may exist whatever the nature of magnetic and electrical order parameters, and they can occur in paramagnetic ferroelectrics, which can be thus classified as multiferroics.<sup>1</sup> Arguably, the most studied multiferroics are based on inorganic oxides, such as perovskite-type  $\text{BiFeO}_3$  and  $\text{BiMnO}_3$ ,<sup>2,3</sup> hexagonal  $\text{RMnO}_3$  ( $R$  = rare earth elements),<sup>4</sup>  $\text{TbMn}_2\text{O}_5$ ,<sup>5</sup> and polar polymorphs of  $\text{ScFeO}_3$ .<sup>6</sup> Single-phase multiferroic materials containing hybrid inorganic–organic frameworks are even rarer than inorganic oxides. Jain et al. reported an example of metal–organic frameworks,  $[(\text{CH}_3)_2\text{NH}_2]\text{Mn}(\text{HCOO})_3$ , with the perovskite  $\text{ABX}_3$  architecture, showing ferroelectric and magnetic phase transitions at 185 and 8.4 K, respectively.<sup>7</sup> Wang et al. discovered a family of multiferroics based on chiral metal–formate frameworks,  $[\text{NH}_4][\text{M}(\text{HCOO})_3]$  ( $M$  = Mn, Fe, Co, and Ni), which display ferroelectric orderings within 191–254 K and antiferromagnetic orderings within 8–30 K.<sup>8</sup>

Why are there so few multiferroics? From a phenomenological view, it is because of mutual exclusion between ferroelectricity and magnetism. For example, most ferroelectrics are insulators, in which transition metal ions have empty  $d$  shells. However, magnetic materials require transition metal ions with partially filled  $d$  shells.<sup>9</sup> Therefore, it seems a great challenge to expand the

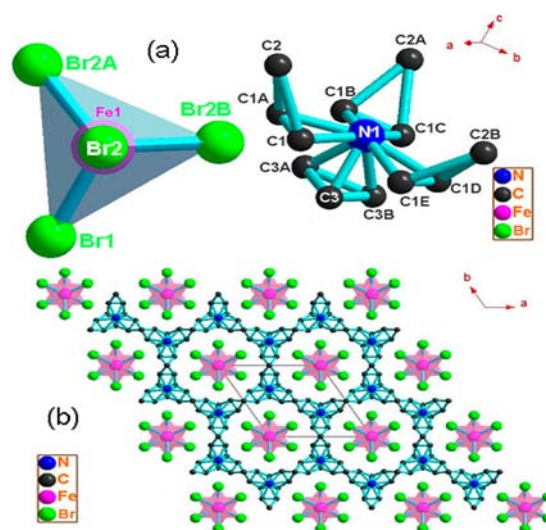


**Figure 1.** (a) Molecular coordination environment and (b) packing diagram of **1** at 293 K. Hydrogen atoms are omitted for clarity.

limited number of multiferroic compounds to gain detailed understanding of rich magnetodielectric phenomena and practical applications. Based on our continuous explorations on molecule-based ferroelectrics,<sup>10</sup> we here present the first organic–inorganic hybrid multiferroic, triethylmethylammonium tetrabromoferrate(III) (**1**), showing strong coupling between ferroelectric and magnetic anomalies or magnetodielectric coupling above room temperature (RT).

Compound **1** was easily obtained as brown-green block single crystals from an aqueous solution containing equimolar  $\text{Et}_3\text{NMeCl}$  and  $\text{FeBr}_3$  with excess  $\text{HBr}$ . It crystallizes in hexagonal space group  $P6_3mc$  at 293 K. The cationic part is completely disordered because the ellipsoid vibrations for all non-hydrogen atoms are not within a reasonable range. Both the  $\text{FeBr}_4^-$  anion and the organic cation lie on a hexagonal axis. The ethyl C1 atom exhibits disorder over two positions with a site occupancy ratio of 1:1. The methyl C3 atom shows a three-fold disorder, with the center of the three sites located on a hexagonal axis (Figure 1a). It

Received: July 26, 2012

Published: October 29, 2012

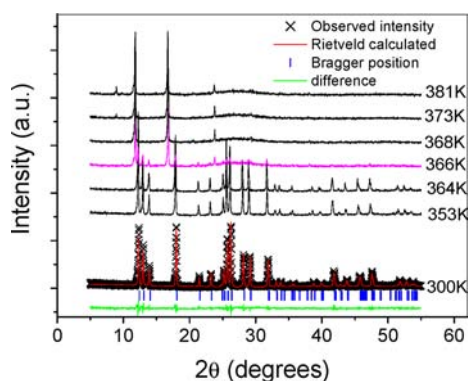


**Figure 2.** PXRD patterns of **1** showing structure phase transition in the temperature range 300–383 K. Rietveld refinement by the GSAS program is shown at the bottom. Black X's indicate the observed XRD intensity at room temperature; the red line is the calculated intensity from the Rietveld refinement; the green line is the difference between them; and blue l's show the Bragg positions.

is interesting to note that the geometry of the cation looks like a slightly distorted trigonal pyramid, similar to the anion. In the crystal lattice, the  $\text{FeBr}_4^-$  anion is surrounded by six cations, showing a typical six-fold symmetry (Figure 1b).

Because it was difficult to obtain a high-temperature (HT) single-crystal structure of **1**, powder X-ray diffraction (PXRD) experiments were performed at HT to reveal structural changes (Figure 2). A clear structural phase transition from ferroelectric (polar space group  $P6_3mc$ ) to paraelectric (centrosymmetry) was observed from the PXRD patterns during the warming process. Below 366 K, the crystal structures were well refined by the Rietveld method with a ferroelectric space group of  $P6_3mc$ . At 366 K (pink line), Bragg diffractions of (100), (200), (101), (102), (110), and (203) planes of the ferroelectric phase were observed, and three new diffraction peaks at  $12.02^\circ$ ,  $17.12^\circ$ , and  $24.32^\circ$  appeared. They belong to a paraelectric phase, indicating coexistence of the ferroelectric and paraelectric phases at this temperature. Above 368 K, only diffractions of the paraelectric phase were observed.

According to the Curie symmetry principle, the paraelectric space group should be the parent space group of the ferroelectric phase. For **1**, the point group of the ferroelectric phase is  $C_{6v}$  (Laue group:  $6mm$ ), and the point group of the paraelectric phase should be  $D_{6h}$  (Laue group:  $6/mmm$ ), which is in good agreement with all of the below-mentioned physical properties measurements.

Interestingly, **1** also undergoes a low-temperature (LT) ferroelectric–ferroelectric phase transition at  $\sim 171$  K with a space group  $P6_3$  (Aizu notation:  $6mmF6$ ), confirmed by differential scanning calorimetry (DSC) and temperature dependence of dielectric constant measurements (see SI).<sup>11</sup> At the same time, the temperature dependence of the second harmonic generation (SHG) effect maintains a non-zero value and displays a small increasing trend near the LT phase transition point (171 K), suggesting the choice of space group  $P6_3$  is reasonable (see SI).

The HT phase transition of **1** was accompanied by thermodynamic anomalies demonstrated by DSC and specific heat measurements. DSC curves (Figure 3) show reversible phase transitions at 368 and 355 K in the warming and cooling processes, respectively. A  $\lambda$ -type peak was observed at 360 K in the specific heat measurement (Figure 3b), which is generally the shape for the first-order phase transition. The phase transition

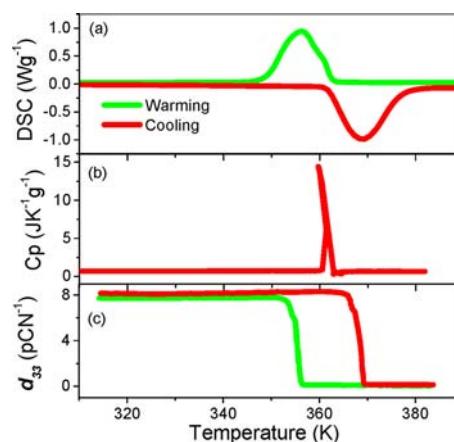


**Figure 3.** Temperature dependence of (a) DSC, (b) specific heat, and (c) piezoelectric coefficient  $d_{33}$  of **1**.

temperature ( $T_c$ ) from the thermodynamic measurements is consistent with that observed from PXRD. The entropy change ( $\Delta S$ ) of the phase transition is estimated from the DSC and heat capacity data to be  $33.7$  and  $15.5 \text{ J K}^{-1} \text{ mol}^{-1}$ , respectively. From the Boltzmann equation,  $\Delta S = R \ln N$ , where  $N$  represents the ratio of possible configurations and  $R$  is the gas constant. It is found that  $N = 58$  and  $7$ , respectively. The large configuration value indicates an extremely high degree of disorder in the crystal structure, which originates from the high disorder of three ethyl groups and one methyl group of the cation.

It is known that all ferroelectrics must have a piezoelectric effect. The piezoelectric matrix for  $6mm$  point group is given as

$$\begin{pmatrix} 0 & 0 & 0 & 0 & d_{15} & 0 \\ 0 & 0 & 0 & d_{15} & 0 & 0 \\ d_{31} & d_{31} & d_{33} & 0 & 0 & 0 \end{pmatrix}$$

At RT the piezoelectric coefficient  $d_{33}$  of **1** is  $\sim 8.0 \text{ pC/N}$ , and it is almost temperature-independent below the  $T_c$  (Figure 3c). Above the  $T_c$ ,  $d_{33}$  decreases to zero quickly, indicating that the crystal structure of **1** changes to a centrosymmetric one, i.e., an occurrence of symmetry breaking with an Aizu notation of  $6/mmmF6mm$ , supported by the HT PXRD measurement.

It is well known that, for a ferroelectric phase transition, a dielectric anomaly is always observed near the  $T_c$  (Figure 4). A step-like dielectric anomaly was observed in **1** at 370 and 347 K in the warming and cooling processes, respectively. This step-like

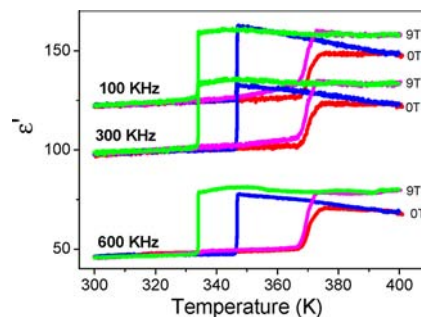


**Figure 4.** Temperature dependence of the real part of the complex dielectric constant of **1** at different frequencies with or without magnetic field. The red and magenta lines and the blue and green lines are measured during warming and cooling processes, respectively.

anomaly of the dielectric constant is a unique characteristic of improper ferroelectrics. According to Landau theory of phase transition, the order parameter of the phase transition of an improper ferroelectric is determined not by the polarization but by another physical quantity. Spontaneous polarization is a secondary effect in improper ferroelectric transitions. At LT **1** has a low dielectric constant, and at HT it has a high one. The dielectric value of the paraelectric phase at 600 kHz is ~40% larger than that of the ferroelectric phase, which gives it potential applications as a “dielectric switch”.<sup>13</sup>

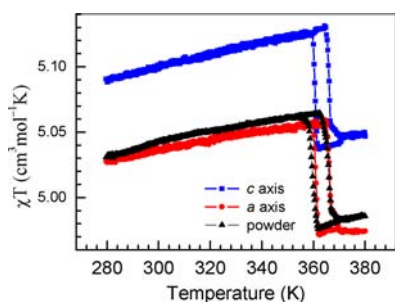


**Figure 5.** Temperature dependence of the magnetic susceptibility of **1** on the magnetic field along the *c*-axis (squares) and *a*-axis (diamond) as well as in powder sample (triangles) during warming (right) and cooling (left) processes.

For most multiferroics, the magnetic phase transition temperature is much lower than the ferroelectric phase transition temperature, resulting in a weak coupling between magnetic and ferroelectric orderings. To probe the possibility of a magnetic phase transition in **1**, magnetic measurements were performed for powder and single-crystal samples with magnetic field parallel to the *a*- or *c*-axis of **1** under a dc field of 1000 Oe (Figure 5). A gradual decrease of the temperature (0.1 K min<sup>-1</sup>) on cooling afforded a steep increase in the  $\chi T$  products with  $T_{1/2\downarrow} = 361$  K. In contrast, upon heating (0.1 K min<sup>-1</sup>), the  $\chi T$  values decreased and returned to the initial value with  $T_{1/2\uparrow} = 366$  K, affording a 5 K thermal hysteresis. This magnetic feature confirmed a reversible structural transformation process that involved transformation between the high-temperature (HT) phase and the low-temperature (LT) phase. The magnetic susceptibility along the *c*-axis is ~1.4% larger than that along the *a*-axis, which means the ferroelectric polarization axis is also the easy magnetization axis.

The calculation for paramagnetic Fe(III) with  $g = 2.00$  and  $S = 5/2$  based on the Brillouin function can completely reproduce the linear  $M-H$  trace, with  $M = 0.131 N\beta$  at 50 kOe, very close to the experimental  $0.14 N\beta$ , suggesting there may be no antiferromagnetic interaction at RT. As Sato points out, an abrupt change in the magnetic susceptibility of transition metal complexes may be attributed to orbital quenching of the angular momentum, instead of control over their spin state.<sup>14</sup> More importantly, this is the first case in which such a sudden jump in the magnetic susceptibility above RT has been reported in molecule-based functional materials, as we are aware that most molecule-based multiferroic systems occur only at very low temperatures.<sup>15</sup> Interestingly, there are also structural phase transitions and magnetic phase transitions occurring at the low temperature of 171 K, but a small magnetic anomaly accompanies a small dielectric constant anomaly (see SI), suggesting there may be a very weak magnetodielectric effect.

Magnetoelectric effect in a single-phase crystal is traditionally described by Landau theory by writing the free energy ( $G$ ) of the system in terms of an applied magnetic field ( $H$ ) and an applied electric field ( $E$ ):<sup>1</sup>

$$-G(E, H) = \frac{1}{2}\epsilon_0\epsilon_{ij}E_iE_j + \frac{1}{2}\mu_0\mu_{ij}H_iH_j + \alpha_{ij}E_iH_j + \alpha_{ij}E_iH_j + \frac{1}{2}\beta_{ijk}E_iH_jH_k + \frac{1}{2}\gamma_{ijk}H_iE_jE_k + \dots$$

The magnetoelectric effect can then be easily established by differentiating  $G$  with respect to  $E_i$  and  $H_i$ . Setting  $E_i = 0$  and  $H_i = 0$ , one gets

$$P_i = \alpha_{ij}H_j + \frac{1}{2}\beta_{ijk}H_jH_k + \dots, \quad \mu_0M = \alpha_{ij}E_j + \frac{1}{2}\gamma_{ijk}E_jE_k + \dots$$

The simultaneous ferroelectric and magnetic phase transitions with the same polarization axis indicate that the coupling between the ferroelectric and magnetic orderings may be very large. Therefore, the dielectric constant of **1** at 9 T magnetic field was determined, and the large magnetic and ferroelectric coupling was confirmed (Figure 6). The dielectric constants at 9 T increase largely, particularly in the paraelectric phase, compared with those without magnetic field. In the warming process the transition temperature is almost unchanged. However, in the cooling process the transition temperatures for all frequencies at 9 T are ~13.1 K lower than those without magnetic field. The magnetodielectric ratio is defined as  $MD \equiv [\epsilon'(\mu_0H) - \epsilon'(0)]/\epsilon'(0)$ . As shown in Figure 6, the MD in the paraelectric phase is larger than that in the ferroelectric phase. Around the  $T_c$ , the MD has its maximum value. The largest MD value is ~18% at 600 kHz, unprecedented in molecular multiferroic systems. Because there is a spin–lattice coupling, the resulting magnetodielectric effect should lead to a multiferroic effect.<sup>16</sup> In contrast, the dielectric constant of  $[(\text{CH}_3)_2\text{NH}_2]\text{Mn}(\text{HCOO})_3$  is nearly unchanged at 5 T, except that the transition temperature decreases 10 K under the magnetic field, indicating the coupling between ferroelectricity and magnetism is very weak since the magnetic transition temperature (8.4 K) is much lower than the ferroelectric transition temperature (185 K).<sup>7</sup>

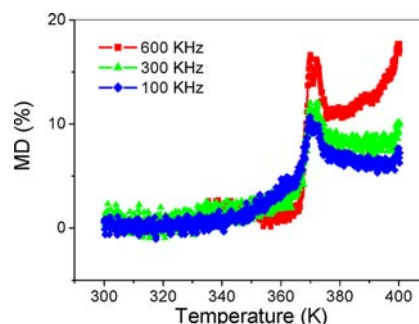


**Figure 6.** Temperature dependence of MD effect of **1** in the warming process.

The observation of a pyroelectric current below the  $T_c$  provides definitive and strong evidence of ferroelectricity of **1**. As shown in Figure 7, spontaneous polarization ( $P_s$ ) exhibits a sharp increase below 367 K, as expected for a ferroelectric phase transition. A maximum polarization of ~0.9  $\mu\text{C}/\text{cm}^2$  was obtained, comparable to those of similar ferroelectrics.<sup>11,15</sup> The step-like shape of the dielectric anomaly and the typical shape of the polarization curve are clear evidence of a ferroelectric

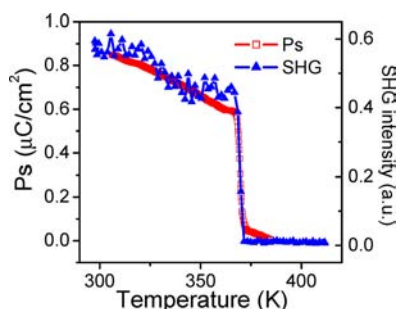


**Figure 7.** Temperature dependence of spontaneous polarization and SHG effect of **1**, showing the critical behaviors in the vicinity of the phase transition temperature. The near overlap of  $P_s$  and SHG curves at the  $T_c$  suggests a good agreement with Landau theory.<sup>10b,c</sup>

transition. Furthermore, the temperature-dependent second-order nonlinear optical susceptibility ( $\chi^{(2)}$ ) also displays a step-like change near the  $T_c$ , suggesting that this phase transition should be of first order; the abrupt change of  $\chi^{(2)}$  from zero to a detectable value firmly testifies that the high-temperature phase must be centrosymmetric. Thus, the change from a centrosymmetric to a non-centrosymmetric transition should be related to the symmetry breaking, in good agreement with the temperature dependence of the piezoelectric coefficient  $d_{33}$ . The relationship between  $P_s$  and  $\chi^{(2)}$  also abides by the Landau theory equation,  $\chi^{(2)} = 6\epsilon_0\beta'P_s$ , where the  $\epsilon_0$  and  $\beta'$  are temperature-independent, suggesting that the HT phase transition should be of first order and a paraelectric-to-ferroelectric one.<sup>10c,17</sup>

In conclusion, the combination of disordered cation and magnetic transition metal ion results in formation of a magnetodielectric molecule-based functional material above room temperature. It will open up a new avenue for multiferroic systems.

## ■ ASSOCIATED CONTENT

### ● Supporting Information

Experimental details and CIF files. This material is available free of charge via the Internet at <http://pubs.acs.org>.

## ■ AUTHOR INFORMATION

### Corresponding Author

xiongrg@seu.edu.cn

### Notes

The authors declare no competing financial interest.

## ■ ACKNOWLEDGMENTS

This work was supported by National Natural Science Foundation of China (20931002, 90922005, and 21101026). We sincerely thank the referees for their excellent magnetic property assignments.

## ■ REFERENCES

- (1) (a) Eerenstein, W.; Mathur, N. D.; Scott, J. F. *Nature* **2006**, *422*, 759. (b) Ponomarev, B. K.; Ivanov, S. A.; Popov, Yu. F.; Negrii, V. D.; Redkin, B. S. *Ferroelectrics* **1994**, *161*, 43.
- (2) Wang, J.; Neaton, J. B.; Zheng, H.; Nagarajan, V.; Ogale, S. B.; Liu, B.; Viehland, D.; Vaithyanathan, V.; Schlom, D. G.; Waghmare, U. V.; Spaldin, N. A.; Rabe, K. M.; Wuttig, M.; Ramesh, R. *Science* **2003**, *299*, 1719.
- (3) (a) Kimura, T.; Kawamoto, S.; Yamada, I.; Azuma, M.; Takano, M.; Tokura, Y. *Phys. Rev. B* **2003**, *67*, 180401. (b) Claridge, J. B.; Hughes, H.; Bridges, C. A.; Allix, M.; Suchomel, M. R.; Niu, H.; Kuang, X.;

Rosseinsky, M. J.; Bellido, N.; Grebille, D.; Perez, O.; Simon, C.; Pelloquin, D.; Blundell, S. J.; Lancaster, T.; Baker, P. J.; Pratt, F. L.; Halasyamani, P. S. *J. Am. Chem. Soc.* **2009**, *131*, 14000. (c) Imamura, N.; Karppinen, M.; Motohashi, T.; Fu, D. S.; Itoh, M.; Yamauchi, H. *J. Am. Chem. Soc.* **2008**, *130*, 14948.

(4) (a) Katsufuji, T.; Mori, S.; Masaki, M.; Moritomo, Y.; Yamamoto, N.; Takagi, H. *Phys. Rev. B* **2001**, *64*, 104419. (b) Fiebig, M.; Lottermoser, T. H.; Fröhlich, D.; Goltsev, A. V.; Pisarev, R. V. *Nature* **2002**, *419*, 818. (c) Ishiwata, S.; Tokunaga, Y.; Taguchi, Y.; Tokura, Y. *J. Am. Chem. Soc.* **2011**, *133*, 13818.

(5) Hur, N.; Park, S.; Sharma, P. A.; Ahn, J. S.; Guha, S.; Cheong, S.-W. *Nature* **2004**, *429*, 392.

(6) Li, M. R.; Adem, U.; McMitchell, S. R. C.; Xu, Z. L.; Thomas, C. I.; Warren, J. E.; Giap, D. V.; Niu, H. J.; Wan, X. M.; Palgrave, R. G.; Schiffmann, F.; Cora, F.; Slater, B.; Burnett, T. L.; Cain, M. G.; Abakumov, A. M.; van Tendeloo, G.; Thomas, M. F.; Rosseinsky, M. J.; Claridge, J. B. *J. Am. Chem. Soc.* **2012**, *134*, 3737.

(7) Jain, P.; Ramachandran, V.; Clark, R. J.; Zhou, H. D.; Toby, B. H.; Dalal, N. S.; Kroto, H. W.; Cheetham, A. K. *J. Am. Chem. Soc.* **2009**, *131*, 13625.

(8) Xu, G. C.; Zhang, W.; Ma, X. M.; Chen, Y. H.; Zhang, L.; Cai, H. L.; Wang, Z. M.; Xiong, R. G.; Gao, S. *J. Am. Chem. Soc.* **2011**, *133*, 14948.

(9) (a) Hill, N. A. *J. Phys. Chem. B* **2000**, *104*, 6694. (b) Cheong, S.-W.; Mostovoy, M. *Nat. Mater.* **2007**, *6*, 13.

(10) (a) Zhang, Y.; Zhang, W.; Li, S. H.; Ye, Q.; Cai, H. L.; Deng, F.; Xiong, R. G.; Huang, S. P. D. *J. Am. Chem. Soc.* **2012**, *134*, 11044. (b) Cai, H.-L.; Zhang, W.; Ge, J.-Z.; Zhang, Y.; Awaga, K.; Nakamura, T.; Xiong, R.-G. *Phys. Rev. Lett.* **2011**, *107*, 147601. (c) Fu, D.-W.; Zhang, W.; Cai, H.-L.; Zhang, Y.; Ge, J.-Z.; Xiong, R.-G.; Huang, S. D. *J. Am. Chem. Soc.* **2011**, *133*, 12780. (d) Zhang, W.; Ye, H.-Y.; Xiong, R.-G. *Coord. Chem. Rev.* **2009**, *253*, 2980. (e) Fu, D.-W.; Zhang, W.; Cai, H.-L.; Zhang, Y.; Ge, J.-Z.; Xiong, R.-G.; Huang, S. D.; Takayoshi, N. *Angew. Chem., Int. Ed.* **2011**, *50*, 11947. (f) Fu, D.-W.; Zhang, W.; Cai, H.-L.; Ge, J.-Z.; Zhang, Y.; Xiong, R.-G. *Adv. Mater.* **2011**, *23*, 5658.

(11) Crystal data of **1**: At  $T = 363$  K,  $C_2H_8NBr_4Fe$ , brown-green block,  $0.40 \times 0.25 \times 0.25$  mm,  $M_r = 491.71$ , hexagonal,  $P6_3mc$ ,  $a = b = 8.344(9)$  Å,  $c = 13.670(2)$  Å,  $\gamma = 120^\circ$ ,  $V = 824.1(2)$  Å<sup>3</sup>,  $Z = 2$ ,  $D_{\text{calc}} = 1.982$  mg m<sup>-3</sup>,  $\mu = 10.582$  mm<sup>-1</sup>,  $S = 1.139$ ,  $R(F) = 0.0813$ ,  $wR(F^2) = 0.1869$ . At  $T = 293$  K, hexagonal,  $P6_3mc$ ,  $a = b = 8.265(9)$  Å,  $c = 13.539(2)$  Å,  $\gamma = 120^\circ$ ,  $V = 800.9(2)$  Å<sup>3</sup>,  $Z = 2$ ,  $D_{\text{calc}} = 2.039$  mg m<sup>-3</sup>,  $\mu = 10.888$  mm<sup>-1</sup>,  $S = 1.103$ ,  $R(F) = 0.0648$ ,  $wR(F^2) = 0.1638$ . At  $T = 243$  K, hexagonal,  $P6_3mc$ ,  $a = b = 8.267(2)$  Å,  $c = 13.524(2)$  Å,  $\gamma = 120^\circ$ ,  $V = 800.4(2)$  Å<sup>3</sup>,  $Z = 2$ ,  $D_{\text{calc}} = 2.040$  mg m<sup>-3</sup>,  $\mu = 10.895$  mm<sup>-1</sup>,  $S = 1.106$ ,  $R(F) = 0.0612$ ,  $wR(F^2) = 0.1639$ . At  $T = 203$  K, hexagonal,  $P6_3mc$ ,  $a = b = 8.169(7)$  Å,  $c = 13.411(3)$  Å,  $\gamma = 120^\circ$ ,  $V = 775.1(9)$  Å<sup>3</sup>,  $Z = 2$ ,  $D_{\text{calc}} = 2.107$  mg m<sup>-3</sup>,  $\mu = 11.251$  mm<sup>-1</sup>,  $S = 1.145$ ,  $R(F) = 0.0557$ ,  $wR(F^2) = 0.1594$ . At  $T = 153$  K, hexagonal,  $P6_3$ ,  $a = b = 16.406(4)$  Å,  $c = 13.519(2)$  Å,  $\gamma = 120^\circ$ ,  $V = 3151.3(9)$  Å<sup>3</sup>,  $Z = 8$ ,  $D_{\text{calc}} = 2073$  mg m<sup>-3</sup>,  $\mu = 11.609$  mm<sup>-1</sup>,  $S = 1.487$ ,  $R(F) = 0.1378$ ,  $wR(F^2) = 0.4237$ .

(12) (a) Hang, T.; Zhang, W.; Ye, H.-Y.; Xiong, R.-G. *Chem. Soc. Rev.* **2011**, *40*, 3577. (b) Zhang, W.; Xiong, R.-G. *Chem. Rev.* **2012**, *112*, 1163.

(13) Zhang, W.; Cai, Y.; Xiong, R. G.; Yoshikawa, H.; Awaga, K. *Angew. Chem., Int. Ed.* **2010**, *49*, 6608.

(14) Juhasz, G.; Matsuda, R.; Kanegawa, S.; Inoue, K.; Sato, O.; Yoshizawa, K. *J. Am. Chem. Soc.* **2009**, *131*, 4560.

(15) (a) Cui, H.; Wang, Z.; Takahashi, K.; Okano, Y.; Kobayashi, H.; Kobayashi, A. *J. Am. Chem. Soc.* **2006**, *128*, 15074. (b) Samantaray, R.; Clark, R. J.; Choi, E. S.; Zhou, H.; Dalal, N. S. *J. Am. Chem. Soc.* **2011**, *133*, 3792.

(16) (a) Lee, J. H.; et al. *Nature* **2010**, *469*, 954. (b) Katsufuji, T.; Takagi, H. *Phys. Rev. B* **2001**, *64*, 054415. (c) Shvartsman, V. V.; Borisov, P.; Kleemann, W.; Kamba, S.; Katsufuji, T. *Phys. Rev. B* **2010**, *81*, 064426. (d) Ghalsasi, P. S.; Inoue, K. *Polyhedron* **2009**, *28*, 1864.

(17) Cai, H.-L.; Fu, D.-W.; Zhang, Y.; Zhang, W.; Xiong, R.-G. *Phys. Rev. Lett.* **2012**, *109*, 169601.